Applied Catalysis B: Environmental 91 (2009) 21–29

Contents lists available at ScienceDirect

Applied Catalysis B: Environmental

journal homepage: www.elsevier.com/locate/apcatb

Intrazeolite cobalt(0) nanoclusters as low-cost and reusable catalyst for hydrogen generation from the hydrolysis of sodium borohydride

Murat Rakap, Saim Özkar *

Department of Chemistry, Middle East Technical University, Inonu Bulvari, 06531, Ankara, Turkey

ARTICLE INFO

Article history:
Received 23 December 2008
Received in revised form 29 April 2009
Accepted 1 May 2009
Available online 19 May 2009

Keywords:
Zeolite
Cobalt
Nanoclusters
Sodium borohydride
Hydrolysis
Hydrogen

ABSTRACT

Intrazeolite cobalt(0) nanoclusters were prepared by ion-exchange of Co^{2+} ions with the extraframework Na^+ ions in the zeolite-Y followed by the reduction of Co^{2+} ions in the supercages of zeolite-Y with sodium borohydride at room temperature. The intrazeolite cobalt(0) nanoclusters were isolated as solid materials and characterized by ICP-OES, XRD, HRTEM, SEM, XPS, Raman spectroscopy and N_2 adsorption technique. The catalytic activities of intrazeolite cobalt(0) nanoclusters in the hydrolysis reaction of sodium borohydride solution in the absence or presence of added base were studied. They are found to be more active in basic solution than in aqueous solution without added base. They provide 36,000 total turnovers and a turnover frequency up to 880 mol H_2 (mol Co)$^{-1}$ h^{-1} in the hydrolysis of basic sodium borohydride solution at 25.0 ± 0.1 °C. The improved hydrogen generation rate, hydrogen generation efficiency, lower activation energy and the low cost make the intrazeolite cobalt(0) nanoclusters promising candidate as catalyst for the hydrogen generation from basic sodium borohydride solution.

1. Introduction

Because of depletion of fossil fuel resources, environmental pollution and global warming caused by a steep increase in carbon dioxide and other greenhouse gases in the atmosphere, there has been an increasing demand for the renewable energy sources, on the way towards a sustainable energy future [1–4]. Hydrogen has been considered as a clean and environmentally benign new energy carrier for heating, transportation, mechanical power and electricity generation [5,6]. Various kinds of solid materials including the alkaline or alkaline earth metal hydrides (CaH_2, LiH, $NaBH_4$, MgH_2, $LiAlH_4$, etc.) [7] have been considered as hydrogen storage material. Among these chemical hydrides, sodium borohydride ($NaBH_4$) has received the most extensive attention owing to its combined advantages of: (i) the high hydrogen storage capacity (10.8 wt.%); (ii) the high stability and no flammability of its alkaline solutions; (iii) the optimal control on hydrogen generation rate by supported catalysts; (iv) the acceptable hydrogen generation rate even at low temperature; (v) the availability and easy handling [8]; (vi) an efficient hydrogen source which releases hydrogen gas in the amount double of its hydrogen content upon hydrolysis in water (Eq. (1)) [9]:

$$NaBH_4(aq) + 2H_2O(l) \xrightarrow{\text{catalyst}} NaBO_2(aq) + 4H_2(g) \quad (1)$$

Although the self-hydrolysis of sodium borohydride at room temperature is quite slow, it can be completely suppressed by working in highly basic solution [10]. Thus, the hydrolysis of sodium borohydride occurs only in the presence of a suitable catalyst [11]. Many transition metals or their compounds have been tested as catalyst for this important reaction [9,12]. Usually, precious metals such as Pt [13], Ru [14], and Pt–Ru alloy [15] provide high activity in the hydrogen generation from the hydrolysis of sodium borohydride, whereby their high cost appears to be a big impediment for their broad applications. Recently, some low-cost metals and alloys, including $LaNi_{4.5}T_{0.5}$ (T = Mn, Cr, Co, Fe, Cu, Al) [16], nickel and cobalt [17], nickel boride [18] and cobalt boride [19] have also been shown to catalyze the hydrolysis of sodium borohydride solution to generate pure hydrogen. However, the low-cost catalysts normally show relatively low activities compared to the precious metal catalysts. For practical uses, the development of low-cost and highly efficient catalysts is desired. As the catalytic activity in heterogeneous catalysis is directly related to the particle size and dispersion degree of the catalyst, the use of small size and highly dispersed particles can make the catalysts contact with the reactant sufficiently, increase the reaction rate and decrease the amount of the catalyst used [20]. Thus, the use of metal nanoclusters with controllable sizes and large surface areas provides a potential route to the preparation of highly active catalysts. Indeed, recent studies [14,21] have shown that using water dispersible transition metal(0) nanoclusters is a promising way to increase the catalytic activity in the hydrolysis of sodium borohydride as the activity of heterogeneous catalyst is

* Corresponding author. Tel.: +90 312 210 3212; fax: +90 312 210 3200.
E-mail address: sozkar@metu.edu.tr (S. Özkar).

0926-3373/$ – see front matter © 2009 Published by Elsevier B.V.
doi:10.1016/j.apcatb.2009.05.014

directly related to its surface area. Despite their high catalytic activity, a big hurdle in the catalytic applications of transition metal nanoclusters is the aggregation of nanoclusters into clumps and ultimately to the bulk metal. This tendency of transition metal nanoclusters leads to a decrease in catalytic activity despite of using the best stabilizers [22]. The use of microporous and mesoporous materials with ordered porous structures as host to encapsulate metal particles has attracted particular interest in catalysis because the framework stabilization can hinder the aggregation of transition metal nanoclusters and the pore size restriction could limit the growth or sintering of the nanoclusters even at high temperatures [23]. Zeolite-Y is considered as a suitable host providing highly ordered large cavities (supercages) with a diameter of 1.3 nm [24]. The most widely used method to generate the metal nanoclusters inside the zeolite pores is to introduce metal cations into the zeolite by ion-exchange and then to treat the ion-exchanged zeolite with a reducing agent such as gaseous H_2 at high temperatures. However, this high temperature treatment may either destruct the zeolite framework or lead to the migration of a large portion of metal atoms out of the zeolite cages [25]. Using a stronger reducing agent than H_2 such as sodium borohydride is expected to facilitate the reduction of metal cations in the zeolite cages at lower temperature. However, the chemistry of the borohydride reduction of non-noble metals is quite complicated. The reaction conditions such as the concentrations of reactants and the atmosphere may determine both the particle size and the identity of the main product. In aqueous solutions, the reduction of Co^{2+} with $NaBH_4$ yields Co_2B as the primary product if the product is handled under anaerobic conditions [26], while the Co_2B is converted to metallic Co particles and boron oxide under aerobic conditions [27]. In this paper, we report the preparation of cobalt(0) nanoclusters within the supercages of zeolite-Y by using the two steps procedure developed for intrazeolite ruthenium(0) nanoclusters [28]: cobalt(II) ions are introduced to the supercages of zeolite-Y by ion-exchange [29] and, then, reduced by sodium borohydride forming the cobalt(0) nanoclusters within the cages of zeolite-Y whereby the zeolite is reloaded by sodium cations. A multiprong approach using advanced analytical techniques was used to characterize the intrazeolite cobalt(0) nanoclusters, which are found to be highly active catalyst in the hydrolysis of sodium borohydride. Hydrogen generation from the hydrolysis of sodium borohydride was studied depending on the cobalt loading of zeolite-Y, catalyst concentration, substrate concentration, temperature and basicity of the medium.

2. Experimental

2.1. Materials

Cobalt(II) nitrate hexahydrate (98+%), sodium borohydride (99%) and sodium zeolite-Y (Si/Al = 2.5) were purchased from Sigma–Aldrich. All chemicals were used as received. Deionized water was distilled by water purification system (Şimşek SL-200, Ankara, Turkey). All glassware and Teflon-coated magnetic stir bars were cleaned with acetone, followed by copious rinsing with distilled water before drying in an oven at 100 °C.

2.2. Preparation of Co(II)-exchanged zeolite-Y (Co^{2+}-Y)

The sodium form of zeolite-Y (1 g) was added to a solution of $Co(NO_3)_2{\cdot}6H_2O$ in 100 mL H_2O in a 250 mL round bottom flask. This slurry was stirred at room temperature for 3 days until the supernatant solution became colorless. After filtration, the Co^{2+}-exchanged zeolite-Y was washed thoroughly with deionized water (3×20 mL) and dried under vacuum. The cobalt content of the Co^{2+}-exchanged zeolite-Y samples was determined by ICP-OES analysis.

2.3. In situ preparation of intrazeolite cobalt(0) nanoclusters and their catalytic activities in the hydrolysis of sodium borohydride

The intrazeolite cobalt(0) nanoclusters were generated in situ from the reduction of the Co^{2+}-exchanged zeolite-Y with sodium borohydride and their catalytic activity was determined by measuring hydrogen generation in the hydrolysis of sodium borohydride. Before starting the formation of cobalt(0) nanoclusters and their catalytic activity test, a jacketed reaction flask (75 mL) containing a Teflon-coated stir bar was placed on a magnetic stirrer (Heidolph MR-301) and thermostated to 25.0 ± 0.1 °C by circulating water through its jacket from a constant temperature bath. Then, a graduated glass tube (50 cm in height and 5.0 cm in diameter) filled with water was connected to the reaction flask to measure the volume of the hydrogen gas to be evolved from the reaction. Next, 284 mg (7.47 mmol) $NaBH_4$ was dissolved in 50 mL water (corresponding to 30 mmol = 672 mL H_2 at 25.0 ± 0.1 °C and 0.91 atm pressure). The solution was transferred with a 50 mL glass-pipette into the reaction flask thermostated at 25.0 ± 0.1 °C. Then, cobalt-exchanged zeolite-Y (Co^{2+}-Y) sample was added into the reaction flask. Cobalt(II) ions were reduced and the cobalt(0) nanoclusters were formed within the supercages of zeolite-Y initiating the hydrolysis reaction of sodium borohydride. Under such circumstances, instead of cobalt borides, metallic cobalt and boron oxide are expected to be the main products [27]. The volume of hydrogen gas evolved was measured by recording the displacement of water level every 5 min at constant atmospheric pressure of 693 Torr. The pH of the solution was recorded to be 9.6 at the beginning of reaction and increased to its final value of 10.8 when all sodium borohydride was converted to sodium metaborate.

2.4. $Na_{56}Y$ catalyzed hydrolysis of sodium borohydride in aqueous medium

To investigate the effect of the host material zeolite-Y on the catalytic activity of intrazeolite cobalt(0) nanoclusters, the hydrolysis of sodium borohydride was performed in the presence of zeolite-Y. Sodium borohydride (284 mg, $[NaBH_4] = 150$ mM) was dissolved in 50 mL water and the solution was transferred with a 50 mL pipette into the reaction flask thermostated at 25.0 ± 0.1 °C, then 688 mg zeolite-Y (corresponds to the maximum amount of zeolite-Y that is used as a host material for all tests reported here) was added to the solution. The reaction flask was closed and the reaction was started. The same experiment was repeated at various temperatures in the range 25–45 °C in order to determine the effect of temperature on the zeolite-Y catalyzed hydrolysis of sodium borohydride.

2.5. Effect of cobalt loading on hydrogen generation rate

In a series of experiments, the catalytic activities of intrazeolite cobalt(0) nanoclusters ([Co] = 2 mM) with 0.20, 0.40, 0.85, 1.68, 2.52, 3.18, 4.14 wt.% cobalt loading were tested in the hydrolysis of 50 mL of 150 mM (284 mg) aqueous sodium borohydride solution in order to determine the effect of cobalt loading on the hydrogen generation rate. All the experiments were performed in the same way as described in Section 2.3 and the catalyst with the best catalytic activity was determined.

2.6. Kinetic study of the hydrolysis of sodium borohydride catalyzed by intrazeolite cobalt(0) nanoclusters in aqueous medium

In order to establish the rate law for catalytic hydrolysis of $NaBH_4$ using intrazeolite cobalt(0) nanoclusters (with 0.85 wt.% cobalt loading) as catalyst, two different sets of experiments were performed in the same way described in Section 2.3. In the first set

of experiments, the hydrolysis reaction was carried out starting with different initial concentration of intrazeolite cobalt(0) nanoclusters (1, 1.5, 2, 2.5 and 3 mM) and keeping the initial sodium borohydride concentration constant at 150 mM. The second set of experiments were carried out by keeping the initial concentration of intrazeolite cobalt(0) nanoclusters constant at 2 mM and varying the $NaBH_4$ concentration of 150, 300, 450, 600 and 750 mM. In all of these experiments, the initial pH of the solution was recorded to be same (pH = 9.6) as in the self-hydrolysis of sodium borohydride. Finally, the catalytic hydrolysis of sodium borohydride was carried out in the presence of intrazeolite cobalt(0) nanoclusters at constant $NaBH_4$ (150 mM) and catalyst (2 mM Co) concentrations at various temperatures in the range 25–45 °C in order to obtain the activation energy (E_a), enthalpy ($\Delta H^{\#}$) and entropy ($\Delta S^{\#}$).

2.7. Effect of sodium hydroxide concentration on hydrogen generation rate

In order to study the effect of NaOH concentration on the catalytic activity of intrazeolite cobalt(0) nanoclusters in the hydrolysis of sodium borohydride (150 mM), catalytic activity tests were carried out at 25.0 ± 0.1 °C by changing the concentration of NaOH (0, 5, 10, 15, and 20 wt.%). In all the experiments, the total volume of solution was kept constant at 50 mL. All the experiments were performed in the same way as described in Section 2.3. The highest activity of intrazeolite cobalt(0) nanoclusters in the hydrolysis of sodium borohydride was obtained when 10 wt.% NaOH was used. Thus, the concentration of NaOH of 10 wt.% was selected for the further experiments.

2.8. Kinetic study of the hydrolysis of sodium borohydride catalyzed by intrazeolite cobalt(0) nanoclusters in basic medium

In order to establish the rate law for catalytic hydrolysis of basic $NaBH_4$ solution containing 10 wt.% NaOH using intrazeolite cobalt(0) nanoclusters as catalyst, two different sets of experiments were performed in the same ways described in Section 2.3. In the first set of experiments, the hydrolysis reaction was carried out starting with different initial concentration of intrazeolite cobalt(0) nanoclusters (1, 1.5, 2, 2.5 and 3 mM) and keeping the initial sodium borohydride concentration constant at 150 mM. The second set of experiments were carried out by keeping the initial concentration of intrazeolite cobalt(0) nanoclusters constant at 2 mM and varying the $NaBH_4$ concentration of 150, 300, 450, 600 and 750 mM. Finally, the catalytic hydrolysis of $NaBH_4$ was carried out in the presence of intrazeolite cobalt(0) nanoclusters at constant substrate (150 mM $NaBH_4$) and catalyst (2 mM Co) concentrations at various temperatures in the range 25–45 °C in order to obtain the activation energy (E_a), enthalpy ($\Delta H^{\#}$) and entropy ($\Delta S^{\#}$).

2.9. Catalytic lifetime of intrazeolite cobalt(0) nanoclusters in the hydrolysis of sodium borohydride

The catalytic lifetime of intrazeolite cobalt(0) nanoclusters in the hydrolysis of sodium borohydride in both aqueous and basic media was determined by measuring the total turnover number (TTO). Such a lifetime experiment was started with a 50 mL solution of intrazeolite cobalt(0) nanoclusters containing 2 mM Co (694 mg of Co^{2+}-Y with the 0.85 wt.% cobalt loading), 1.2 M $NaBH_4$ (2.27 g), and 10 wt.% NaOH (only for basic solution) at 25.0 ± 0.1 °C and 0.91 atm pressure. The reaction was continued until no hydrogen gas evolution was observed and then 2.27 g of $NaBH_4$ was added again into the reaction flask. Successive addition of a new batch of $NaBH_4$ was continued until the hydrogen gas evolution rate was slowed down to the level of self-hydrolysis.

2.10. Isolability and reusability of intrazeolite cobalt(0) nanoclusters in the hydrolysis of sodium borohydride in basic medium

For the determination of isolability and reusability of intrazeolite cobalt(0) nanoclusters in the hydrolysis of basic sodium borohydride solution, 284 mg (150 mM) $NaBH_4$, 694 mg (2 mM) Co^{2+}-Y (with the 0.85 wt.% cobalt loading) and 10 wt.% NaOH were used by following the same procedure described in Section 2.3. When the 2 mM intrazeolite cobalt(0) nanoclusters catalyzed hydrolysis of 150 mM $NaBH_4$ in basic solution was completed at 25.0 ± 0.1 °C, the catalyst was isolated by suction filtration, washed three times with 20 mL of deionized water, and dried under nitrogen at room temperature. The dried samples of intrazeolite cobalt(0) nanoclusters were used again in the hydrolysis of 150 mM $NaBH_4$ and the same procedure was repeated five times and results were expressed in terms of remaining percent activity of intrazeolite cobalt(0) nanoclusters in the hydrolysis of basic $NaBH_4$ solution.

2.11. Characterization techniques

The cobalt content of the samples was determined by ICP-OES (Leeman-Direct Reading Echelle). For this purpose, the samples were dissolved in a mixture of nitric acid and hydrochloric acid.

Powder X-ray diffraction (XRD) patterns were recorded with a Rigaku X-ray Diffractometer using Cu Kα radiation (30 kV, 15 mA) at room temperature. Scanning was performed between 0° and 55° 2θ. The measurements were made with 0.01° and 0.05° steps and 1°/min rate. The divergence slit was variable and scattering and receiving slit were 4.2° and 0.3 mm, respectively.

High resolution transmission electron microscopy (HRTEM) analysis was carried out with the expert assistance of Dr. Joan Hudson at Clemson University using a Hitachi H7600T operating at 120 kV and with a 2.0 Å point-to-point resolution. Samples were examined at magnification between 100 and 400 K. One drop of dilute suspension of sample in pentane was deposited on the TEM grids and the solvent was then evaporated.

The X-ray photoelectron spectroscopy (XPS) analysis of the catalyst was performed on a Physical Electronics 5800 spectrometer equipped with a hemispherical analyzer and using monochromatic Al Kα lines of Al (1486.6 eV, 10 mA) as an X-ray source.

The Raman spectra of sample was recorded on Bruker RFS-100/S series Raman spectrometer equipped with Nd-YAG laser at 1064 nm using the FT-Raman technique.

Scanning electron microscopy (SEM) analysis was carried out using a Hitachi S-800 scanning electron microscope operating at an accelerating voltage of 10 kV. SEM samples on quartz surfaces were coated with about 5 nm of Pt/Au alloy.

3. Results and discussion

3.1. Characterization of intrazeolite cobalt(0) nanoclusters

Comparison of the powder XRD patterns of Co^{2+}-exchanged zeolite-Y (Co^{2+}-Y), intrazeolite cobalt(0) nanoclusters (Co(0)-Y) and the starting material ($Na_{56}Y$) shows clearly that no significant structural alteration occurred after the ion-exchange and reduction processes. Moreover, the diffraction peak ascribed to Co_2B alloy (at 45.7°) and cobalt oxide (at 36.8°) did not appear, confirming that metallic cobalt was the main product under our experimental conditions [27].

The crystal morphology of the intrazeolite cobalt(0) nanoclusters was investigated by scanning electron microscopy (SEM) and high resolution transmission electron microscopy (HRTEM). The SEM image of the intrazeolite cobalt(0) nanoclusters (Fig. 1a) shows the hexagonal structure of zeolite-Y crystals, confirming

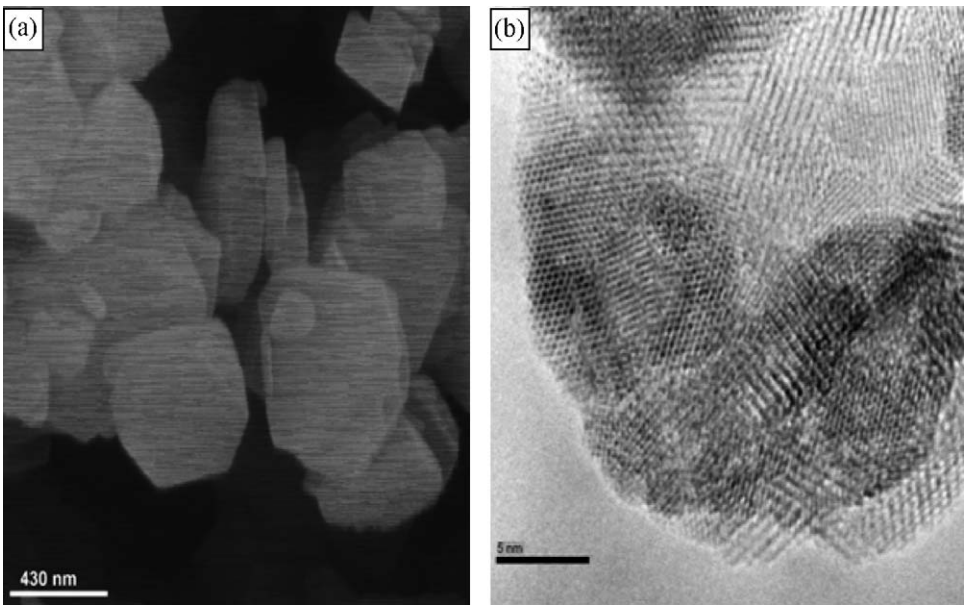

Fig. 1. The typical (a) SEM image and (b) the high resolution TEM micrograph of the intrazeolite cobalt(0) nanoclusters sample harvested after complete hydrolysis of sodium borohydride (50 mL, 150 mM $NaBH_4$).

that the procedures (ion-exchange followed by reduction) for the preparation of intrazeolite cobalt(0) nanoclusters do not cause any changes in the structure of zeolite-Y as observed in the XRD analysis. It also confirms the absence of bulk metal formed on the zeolite surface in detectable sizes. Since the ICP-OES analysis indicates the presence of cobalt in the sample, one can conclude that the cobalt metal is within the cages of zeolite-Y. Indeed, the high resolution TEM image of the same sample given in Fig. 1b shows the uniform distribution of cobalt in the highly ordered cages of zeolite-Y.

Nitrogen adsorption–desorption isotherms of zeolite-Y and the intrazeolite cobalt(0) nanoclusters are shown in Fig. 2. Zeolite-Y showed the type I isotherm, which is typical for microporous materials and the shape of the isotherm did not change after the reduction of Co^{2+}-Y sample with $NaBH_4$ forming intrazeolite cobalt(0) nanoclusters. The absence of a hysteresis loop indicates that there are no mesopores formed in the zeolite structure after reduction. The parameters of the porous structures were calculated from the nitrogen adsorption–desorption isotherms. The formation of cobalt(0) nanoclusters within the supercages of zeolite-Y leads to a decrease in the surface area from 823 to 652 $m^2\ g^{-1}$ and the volume of micropores from 0.332 to 0.294 $cm^3\ g^{-1}$. The decrease in both the surface area and the volume of micropores is due to the encapsulation of cobalt particles in the micropores of zeolite-Y and provides additional evidence for the presence of cobalt(0) nanoclusters within the zeolite cages.

Experimental and simulated X-ray photoelectron spectra (XPS) of the intrazeolite cobalt(0) nanoclusters sample with a cobalt loading of 0.85% are given in Fig. 3 which shows two prominent absorption bands at 780 and 796.3 eV, readily attributable to Co(0) $2p_{3/2}$ and Co(0) $2p_{1/2}$, respectively. Compared to the values for bulk cobalt [30] (778.5 and 794.7 eV), the Co $2p_{3/2}$ and Co $2p_{1/2}$ peaks of intrazeolite cobalt(0) nanoclusters are shifted to higher binding energies by 1.5 and 1.6 eV, respectively. This shift might be attributed to both the quantum size effect and peculiar electronic properties of the zeolite matrix [31]. The interaction of cobalt(0) nanoclusters with the framework oxygen of the zeolite cages is

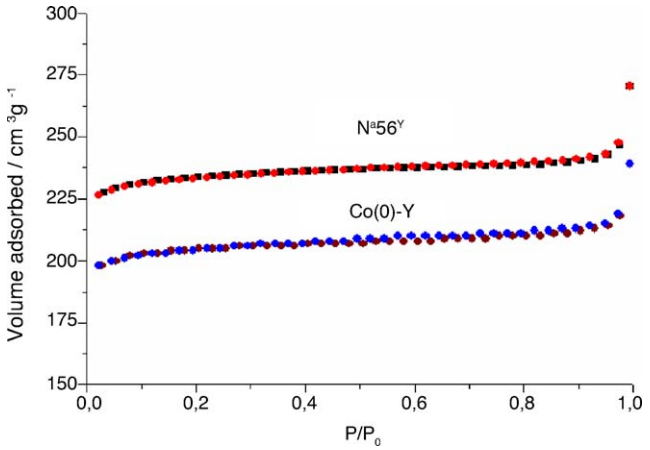

Fig. 2. The N_2 adsorption–desorption isotherms of zeolite-Y ($Na_{56}Y$) and intrazeolite cobalt(0) nanoclusters.

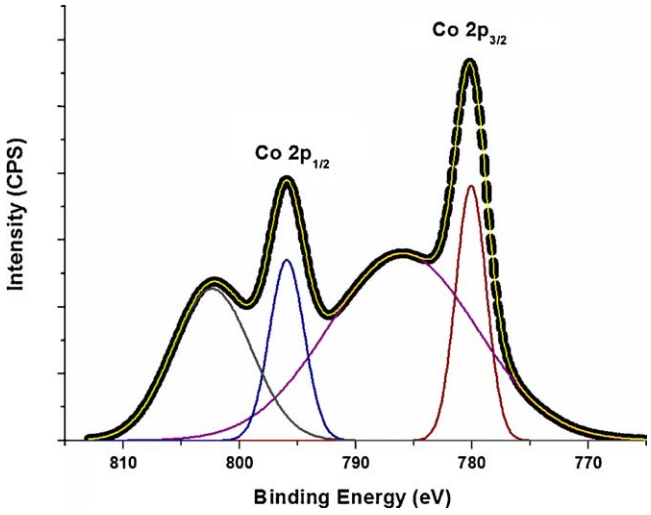

Fig. 3. Experimental and simulated X-ray photoelectron spectra (XPS) of intrazeolite cobalt(0) nanoclusters prepared by the reduction of Co^{2+}-exchanged zeolite-Y.

expected to induce a positive charge on the surface metal, which would increase the binding energies of cobalt(0) nanoclusters [31b]. In addition to the matrix effect, the high energy shift in the cobalt binding energy might be due to the fact that electrons in the core level are strongly restricted by the atomic nucleus, as observed in the case of palladium(0) nanoclusters in zeolite-Y [31d]. The XPS also exhibits two additional slightly higher energy features, which indicate the cobalt oxide formation. Although oxidation of metal nanoclusters during the XPS sampling procedure is a known phenomenon [32], the results obtained from XPS analysis need to be tested by using another spectroscopic technique because there is no indication of cobalt oxide formation in the XRD results. Raman spectroscopy [33] was used to check whether cobalt oxide is really formed during the XPS sampling procedure or in the preparation of intrazeolite cobalt(0) nanoclusters as it is a strong tool to test the existence of cobalt oxides. Raman spectra of zeolite-Y and intrazeolite cobalt(0) nanoclusters do not differ from each other significantly. Furthermore, the characteristic Raman peaks expected for CoO and Co_3O_4 at 691 and 693 cm^{-1} [34] are not seen in the Raman spectrum of intrazeolite cobalt(0) nanoclusters. From these observations, it can be concluded that the cobalt oxide observed in the XPS spectrum is due to surface oxidation of the catalyst during XPS sampling procedure. Moreover, the absence of any absorption band belonging to the boron indicates that the catalyst is composed of metallic cobalt.

3.2. Hydrolysis of sodium borohydride catalyzed by $Na_{56}Y$

To determine the catalytic activity of intrazeolite cobalt(0) nanoclusters more accurately, one has to check whether zeolite-Y catalyzes the hydrolysis of sodium borohydride. The hydrolysis of sodium borohydride in the presence of zeolite-Y was performed at various temperatures in the range 25–45 °C. It was found that the hydrogen generation from the hydrolysis of sodium borohydride in the presence of zeolite-Y increases with the increasing temperature from 1.1 to 4.2 mL H_2/min for 25 and 45 °C, respectively. Although the hydrolysis of sodium borohydride in the presence of zeolite-Y is slow, all of the catalytic activity results of intrazeolite cobalt(0) nanoclusters in the hydrolysis of sodium borohydride given here were corrected by subtracting the amount of hydrogen gas due to the hydrolysis of sodium borohydride in the presence of zeolite-Y from the values of hydrogen gas obtained from the intrazeolite cobalt(0) nanoclusters catalyzed hydrolysis of sodium borohydride.

3.3. Effect of cobalt loading on hydrogen generation rate

Intrazeolite cobalt(0) nanoclusters samples with various cobalt loading were prepared by changing the concentration of cobalt(II) solution in ion-exchange and tested for their catalytic activity in the hydrolysis of aqueous sodium borohydride solution. Fig. 4 shows the variation in the catalytic activity of intrazeolite cobalt(0) nanoclusters with cobalt loading of the zeolite. The variation in catalytic activity reflects the accessibility of cobalt(0) nanoclusters in the zeolite cages by the substrate. The highest catalytic activity is obtained by using the intrazeolite cobalt(0) nanoclusters containing 0.40 wt.% Co, most probably in the supercage (α-cage), where the substrate more readily access cobalt(0) nanoclusters compared to the β-cage of zeolite-Y. As the cobalt loading increases, the nanoclusters might go to the less accessible sodalite cages as well, or nanoclusters in the supercages block the entrance to the supercages becoming larger. In order to keep the cobalt concentration at a certain level in the catalytic reaction using total catalyst in the amount as small as possible, the intrazeolite cobalt(0) nanoclusters catalyst with 0.85 wt.% cobalt loading was selected for the further experiments.

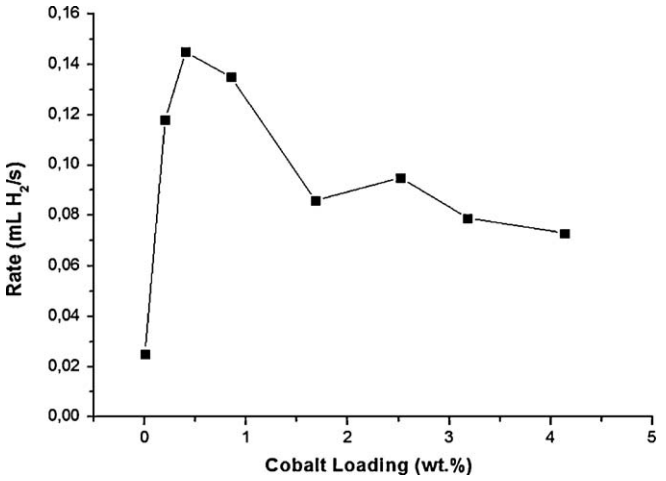

Fig. 4. The rate of hydrogen generation versus cobalt loading (in wt.%) for the hydrolysis of sodium borohydride (50 mL, 150 mM $NaBH_4$) catalyzed by intrazeolite cobalt(0) nanoclusters (2 mM Co) at 25.0 ± 0.1 °C.

3.4. Catalytic activity of intrazeolite cobalt(0) nanoclusters in the hydrolysis of sodium borohydride in aqueous medium

Intrazeolite cobalt(0) nanoclusters were found to be highly active catalyst in the hydrolysis of sodium borohydride liberating hydrogen gas. Fig. 5 shows the plot of the volume of H_2 generated versus time during the catalytic hydrolysis of 150 mM $NaBH_4$ solution in the presence of intrazeolite cobalt(0) nanoclusters in different concentrations at 25.0 ± 0.1 °C. Note that the values for the $Na_{56}Y$ catalyzed hydrolysis of sodium borohydride were subtracted from the values of hydrogen gas obtained from the intrazeolite cobalt(0) nanoclusters catalyzed hydrolysis of sodium borohydride at the same temperature. Plotting the hydrogen generation rate, determined from the linear portion of the plots in Fig. 5, versus cobalt concentration, both in logarithmic scales (the inset in Fig. 5), gives a straight line with a slope of 0.99 ≈ 1.0 indicating that the hydrolysis is first order with respect to the catalyst concentration.

The effect of $NaBH_4$ substrate concentration on the hydrogen generation rate was also studied by performing a series of experiments starting with various initial concentration of $NaBH_4$ in the range 150–750 mM while keeping the catalyst concentration

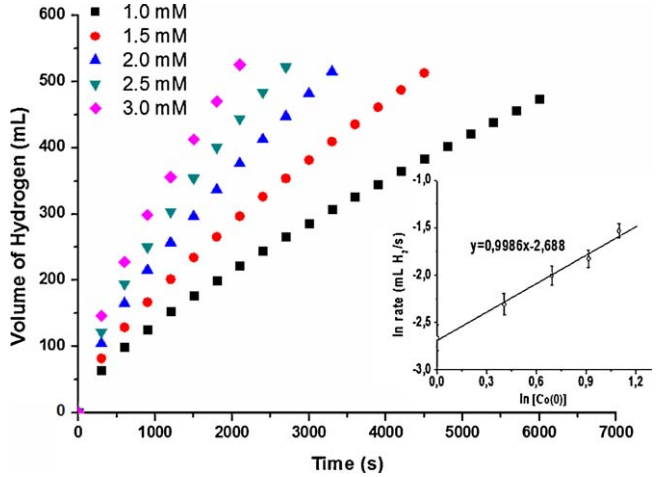

Fig. 5. Plot of the volume of hydrogen (mL) versus time (s) for the hydrolysis of sodium borohydride (50 mL, 150 mM $NaBH_4$) catalyzed by intrazeolite cobalt(0) nanoclusters with different catalyst concentration at 25.0 ± 0.1 °C. Inset: plot of the hydrogen generation rate versus the catalyst concentration (both in logarithmic scale) for the same reactions.

constant at 2 mM Co. The hydrogen generation rate was found to be practically independent of the $NaBH_4$ concentration in the range 150–750 mM indicating that the hydrolysis reaction is zero order with respect to the concentration of $NaBH_4$. Consequently, the rate law for the catalytic hydrolysis of sodium borohydride in aqueous solution can be given as in Eq. (2),

$$-\frac{4d[NaBH_4]}{dt} = \frac{d[H_2]}{dt} = k[Co] \quad (2)$$

The hydrolysis of sodium borohydride catalyzed by intrazeolite cobalt(0) nanoclusters was performed at various temperatures in the range 25–45 °C starting with the initial substrate concentration of 150 mM $NaBH_4$ and an initial catalyst concentration of 2 mM Co. The values of rate constant k determined from the linear portions of the H_2 volume versus time plots at five different temperatures (Fig. 6) were used to calculate the activation parameters for this catalytic hydrolysis of sodium borohydride: activation energy E_a = 55 ± 2 kJ mol^{-1}, activation enthalpy $\Delta H^{\#}$ = 52 ± 2 kJ mol^{-1}, and activation entropy $\Delta S^{\#}$ = −94 ± 4 J K^{-1} mol^{-1}.

3.5. Effect of sodium hydroxide concentration on the hydrogen generation rate

Fig. 7 shows the plot of hydrogen generation rate versus concentration of NaOH in wt.% for the hydrolysis reaction of $NaBH_4$ catalyzed by intrazeolite cobalt(0) nanoclusters. The rate of hydrogen generation first increases with the increasing sodium hydroxide concentration, demonstrating an enhancement of reaction by NaOH. It reaches a maximum value at the concentration of 10 wt.% NaOH and subsequently decreases with the further increase in NaOH concentration. As implied by the plot of catalytic activity versus percentage of sodium hydroxide, all the subsequent experiments were performed in solutions containing 10 wt.% NaOH. A control test was performed to check whether the use of sodium hydroxide causes leaching of cobalt from the catalyst. ICP-OES analysis of the catalyst sample after catalytic reaction in the presence of 10 wt.% NaOH gave the same cobalt content (0.85 wt.% Co) for the intrazeolite nanoclusters as before the reaction.

The integrity of zeolite was tested by taking nitrogen adsorption/desorption isotherms of the intrazeolite cobalt(0) nanoclusters samples isolated from the hydrolysis of sodium borohydride in basic solutions containing sodium hydroxide in different concentrations (wt.% NaOH = 5, 10, 15, 20). The micropore volume and surface area calculated by t-plot method [35] from the nitrogen adsorption–desorption isotherms are given in Table 1. Upon preparation of intrazeolite cobalt(0) nanoclusters in the presence of increasing amount of sodium hydroxide, both the micropore surface area and volume were increased compared to that of the sample prepared in the absence of sodium hydroxide. The increase in both surface area and volume is not significant for the samples prepared in basic solution containing 5 and 10 wt.% NaOH, while significant increase is observed for the samples prepared in solutions containing 15 and 20 wt.% NaOH. This indicates the formation of mesopores in the samples using 15 and 20 wt.% NaOH which is also apparent from the hysteresis loop in the nitrogen adsorption/desorption isotherms for these samples. The removal of a small part of the silicon atoms in the zeolite framework by the attack of hydroxyl ions should mainly be responsible for the formation of mesopores [23a] which might lead to a decrease in the catalytic activity of intrazeolite cobalt(0) nanoclusters in the hydrolysis of basic sodium borohydride solution containing 15 and 20 wt.% NaOH. Consequently, it can be concluded that the rate of hydrogen generation is not only dependent on the nature of the catalyst [18,36] but also on the sodium hydroxide concentration of solution.

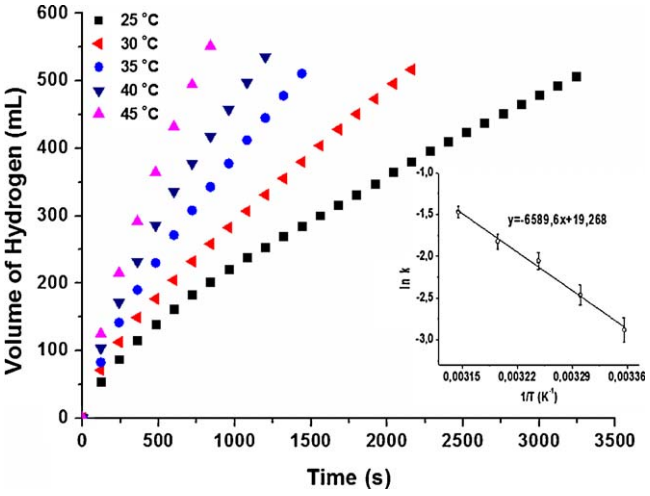

Fig. 6. Plot of the volume of hydrogen (mL) versus time (s) for the hydrolysis of sodium borohydride (50 mL, 150 mM $NaBH_4$) catalyzed by intrazeolite cobalt(0) nanoclusters (2.0 mM Co) at different temperatures (25, 30, 35, 40 and 45 °C). The inset shows the Arrhenius plot.

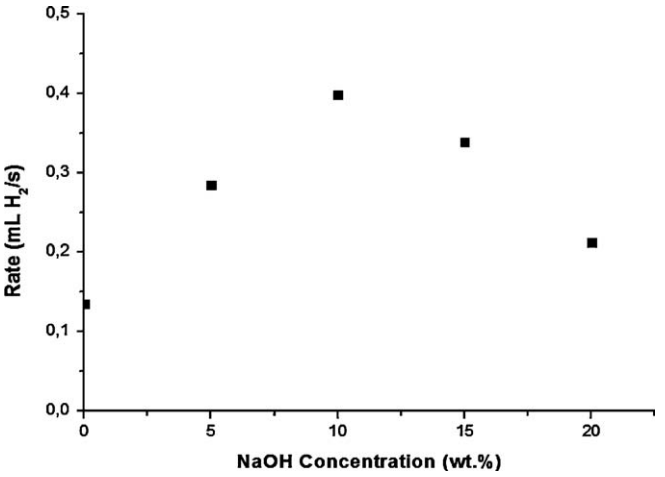

Fig. 7. The plot of hydrogen generation rate versus concentration of NaOH (in wt.%) for the hydrolysis of sodium borohydride (50 mL, 150 mM $NaBH_4$) catalyzed by intrazeolite cobalt(0) nanoclusters (2 mM Co) at 25.0 ± 0.1 °C.

Table 1
Micropore surface area and micropore volume calculated by t-plot method [35] from nitrogen adsorption–desorption isotherms for intrazeolite cobalt(0) nanoclusters prepared in the basic solution containing sodium hydroxide in different concentration.

wt.% NaOH	Surface area (m^2 g^{-1})	Micropore volume (cm^3 g^{-1})
0.0	652	0.294
5.0	671	0.297
10.0	692	0.301
10.0[a]	885	0.363
15.0	831	0.347
20.0	845	0.351

[a] The nanoclusters sample isolated from reusability experiment after fifth run of the hydrolysis of sodium borohydride in a solutions containing 10 wt.% NaOH.

3.6. Catalytic activity of intrazeolite cobalt(0) nanoclusters in the hydrolysis of sodium borohydride in basic medium

The intrazeolite cobalt(0) nanoclusters retain their high catalytic activity in the hydrolysis of sodium borohydride in basic solution. It should be noted that there is no self-hydrolysis or $Na_{56}Y$

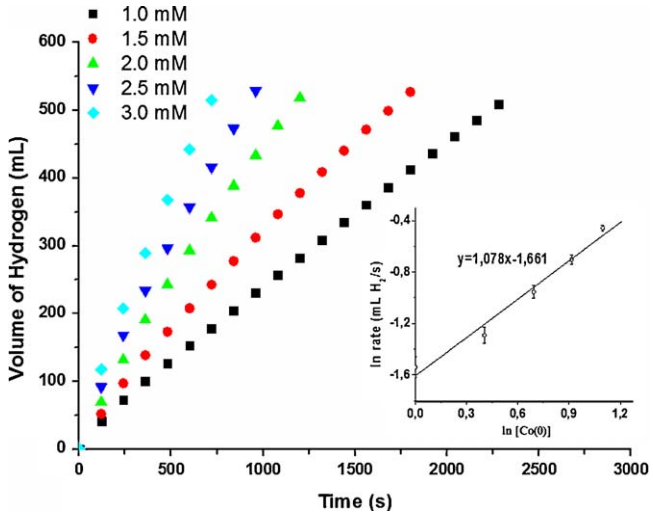

Fig. 8. The volume of hydrogen (mL) versus time (s) plot depending for the hydrolysis of sodium borohydride (50 mL, 150 mM $NaBH_4$) catalyzed by intrazeolite cobalt(0) nanoclusters with various catalyst concentration in basic solution (10 wt.% NaOH) at 25.0 ± 0.1 °C. Inset: plot of the hydrogen generation rate versus the catalyst concentration (both in logarithmic scale) for the same reactions.

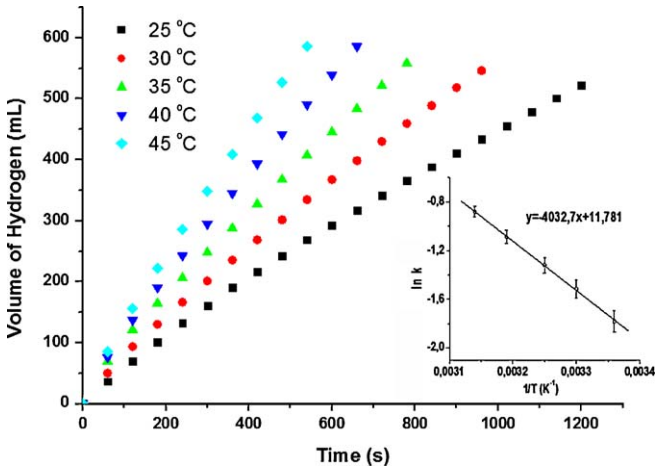

Fig. 9. Plot of the volume of hydrogen (mL) versus time (s) for the hydrolysis of sodium borohydride (50 mL, 150 mM $NaBH_4$) catalyzed by intrazeolite cobalt(0) nanoclusters (2.0 mM Co) in basic solution (10 wt.% NaOH) at different temperatures (25, 30, 35, 40 and 45 °C). The inset shows the Arrhenius plot.

catalyzed hydrolysis in basic solution. Fig. 8 shows the plot of the volume of hydrogen generated versus time during the catalytic hydrolysis of 150 mM $NaBH_4$ solution containing 10 wt.% NaOH in the presence of intrazeolite cobalt(0) nanoclusters in different cobalt concentrations at 25.0 ± 0.1 °C. Plotting the hydrogen generation rate, determined from the linear portion of the plots in Fig. 8, versus cobalt concentration, both in logarithmic scales (the inset in Fig. 8), gives a straight line with a slope of 1.08 ≈ 1.0 indicating that the hydrolysis is first order with respect to the catalyst concentration as in the absence of sodium hydroxide.

The effect of $NaBH_4$ substrate concentration on the hydrolysis rate was also studied by carrying out a series of experiments starting with varying initial concentration of $NaBH_4$ while keeping the catalyst concentration constant at 2 mM Co in the presence of 10 wt.% NaOH. The hydrogen generation rate was found to be practically independent of the $NaBH_4$ concentration also in the presence of 10 wt.% NaOH. This indicates that the hydrolysis reaction is zero order with respect to the concentration of $NaBH_4$ in the presence of sodium hydroxide (10 wt.% NaOH). Consequently, the rate law for the catalytic hydrolysis of sodium borohydride in the presence of 10 wt.% NaOH is the same as given in Eq. (2) for the hydrolysis in the absence of sodium hydroxide.

The hydrolysis of sodium borohydride catalyzed by intrazeolite cobalt(0) nanoclusters in basic solution (10 wt.% NaOH) was carried out at various temperatures in the range 25–45 °C starting with the initial substrate concentration of 150 mM $NaBH_4$ and an initial catalyst concentration of 2 mM Co. The values of rate constant k determined from the linear portions of the H_2 volume versus time plots at five different temperatures (Fig. 9) were used to calculate the activation parameters for the hydrolysis of sodium borohydride in the presence of 10 wt.% NaOH catalyzed by intrazeolite cobalt(0) nanoclusters: activation energy $E_a = 34 \pm 2$ kJ mol^{-1}, activation enthalpy $\Delta H^{\#} = 31 \pm 2$ kJ mol^{-1}, and activation entropy $\Delta S^{\#} = -154 \pm 6$ J K^{-1} mol^{-1}.

Activation energies for the hydrolysis reaction of basic sodium borohydride solution catalyzed by other catalysts and the catalyst used in this study are listed in Table 2 for comparison. Intrazeolite cobalt(0) nanoclusters provide a significantly lower activation energy for the hydrolysis of sodium borohydride in basic solution.

Table 2
Activation energies for different catalyst systems used for the hydrolysis of basic sodium borohydride solution.

Catalyst	E_a (kJ mol^{-1})	Experimental conditions		Reference
		$NaBH_4$	NaOH	
Intrazeolite cobalt(0) nanoclusters	34	0.15 M	10%	This work
Ni–Co–B	62	0.16 g	15%	[36]
Co–B/Ni foam	33	20%	10%	[39]
Ni_xB	38	1.5%	10%	[18a]
Ru/IRA-400	47	20%	10%	[40]
Co/γ-Al_2O_3	33	5%	5%	[12l]
Co/C	46	5%	5%	[12l]
Carbon supported Co–B	58	0.2 M	20 mmol	[20]
Ru-promoted sulphated Zr	76	0.661 M	1.3 M	[41]
Pd–C powder	28	0.005 M	pH = 13	[42]
Ru(0) nanoclusters	43	0.15 M	10%	[14a]
Pt/$LiCoO_2$	70	10%	5%	[43]
Ru/$LiCoO_2$	68	10%	5%	[43]
Ru/IR-120	50	5%	1%	[14b]
BMR07 (Ni based)	52	20%	7%	[44]
Ru/IRA-400	56	7.5%	1%	[11]
Ni210 powder	63	0.2 g	10%	[17a]
Co powder	42	0.2 g	10%	[17a]
CoB	45	25%	3%	[8]
Co–Mn–B nanocomposites	55	5%	5%	[45]
Ru/C	67	0.993 M	3.75%	[46]
PtPd-carbon nanotubes	19	0.015 M	pH = 13	[12r]
Co–P	60	10%	1%	[17b]
Co/AC	44	5%	5%	[17c]
Co–W–B/Ni	29	20%	5%	[18b]

3.7. Catalytic lifetime of intrazeolite cobalt(0) nanoclusters in the hydrolysis of sodium borohydride

A lifetime experiment for the intrazeolite cobalt(0) nanoclusters catalyst in the hydrolysis of sodium borohydride in both aqueous and basic media was started with 2 mM intrazeolite cobalt(0) nanoclusters in 50 mL aqueous solution of sodium borohydride at 25.0 ± 0.1 °C. As it can be seen from Fig. 10, they provide higher total turnover value (36,000) in the presence of 10 wt.% sodium hydroxide than that of aqueous solution (12,000) without added base. They also provide higher turnover frequency (880 mol H_2 (mol Co)$^{-1}$ h^{-1}) in basic solution than that of aqueous solution without added base (250 mol H_2 (mol Co)$^{-1}$ h^{-1}). It should be noted that the catalytic lifetime experiment without added base

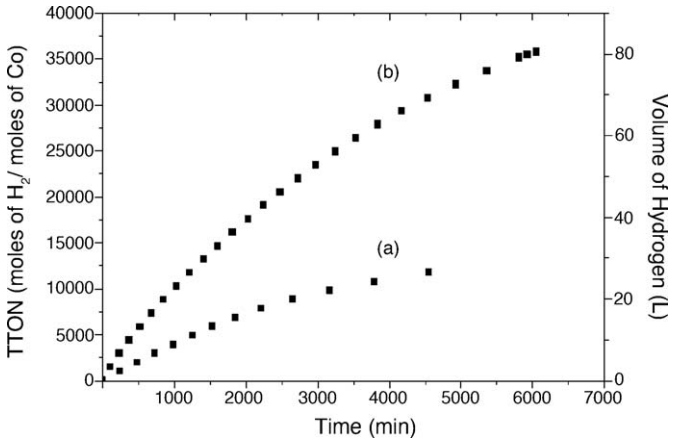

Fig. 10. Graph of total turnover number (TTON) and volume of hydrogen (L) versus time (min) for the hydrolysis of sodium borohydride catalyzed by intrazeolite cobalt(0) nanoclusters (2.0 mM Co) in the absence (a) or presence (b) of added base (10 wt.% NaOH) at 25.0 ± 0.1 °C.

was stopped at earlier stage (around 75 h) when no more hydrogen evolution was observed, perhaps, because of the increasing viscosity of the solution which makes the solution hardly stirred due to the metaborate formation.

3.8. Isolability and reusability of intrazeolite cobalt(0) nanoclusters in the hydrolysis of sodium borohydride in basic medium

Isolability and reusability of the intrazeolite cobalt(0) nanoclusters in the hydrolysis of basic sodium borohydride solution were also tested. A typical experiment was started with 2 mM catalyst in 50 mL aqueous solution of sodium borohydride containing 10 wt.% NaOH at 25.0 ± 0.1 °C. After the complete hydrolysis of 50 mL of 150 mM $NaBH_4$ solution catalyzed by intrazeolite cobalt(0) nanoclusters, the catalyst was isolated by suction filtration, washed with water, and dried under N_2 purging at room temperature. The isolated intrazeolite cobalt(0) nanoclusters are redispersible in basic solution of sodium borohydride, and yet still active catalyst. Fig. 11 shows the percent catalytic activity that retained and the conversion of sodium

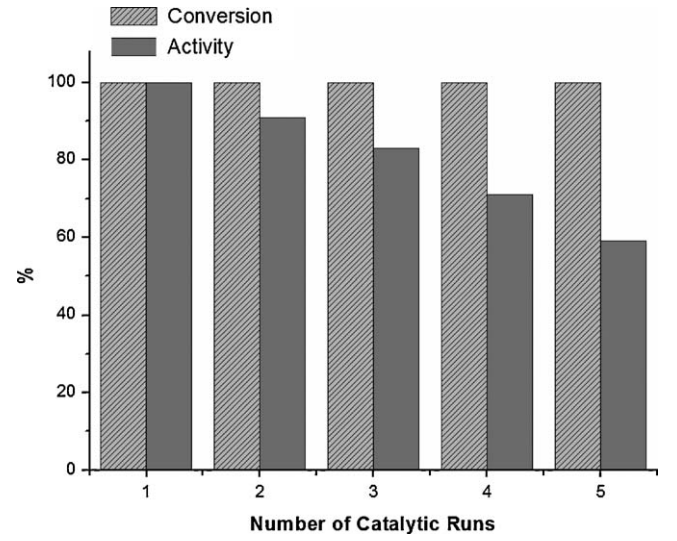

Fig. 11. % Catalytic activity retained and the conversion of sodium borohydride versus number of subsequent catalytic runs for the hydrolysis of sodium borohydride catalyzed by intrazeolite cobalt(0) nanoclusters (2.0 mM Co) in basic solution (10 wt.% NaOH) at 25.0 ± 0.1 °C. (The initial substrate concentration was 150 mM $NaBH_4$ in each run.)

borohydride in the subsequent catalytic runs for the hydrolysis of basic sodium borohydride solution. They retain 59% of their initial catalytic activity after fifth run providing still complete conversion. The activity loss is, in part, due to the decrease in the cobalt content of the sample after fifth run, as determined by ICP-OES analysis performed after fifth run of the catalytic hydrolysis of sodium borohydride in solution containing 10 wt.% NaOH at 25.0 ± 0.1 °C. The cobalt content of 0.85 wt.% for the intrazeolite nanoclusters sample was lowered to 0.76 wt.% after the fifth run in the high concentration of NaOH. The activity loss may be also due to the mesopore formation. Nitrogen adsorption–desorption isotherm of the sample after the fifth run shows an significant increase in both micropore volume and surface area of zeolite (Table 1) indicating the formation of mesopores in that sample. Consequently, the material loss during the isolation and redispersing procedures, passivation of nanoclusters surface by increasing amount of boron products, e.g. metaborate, which might decrease the accessibility of active sites [37,38] or the decrease in the cobalt content of the catalyst should be responsible for the decrease in the activity of the catalyst in subsequent catalytic runs. Despite this activity loss, it can be concluded that the intrazeolite cobalt(0) nanoclusters are isolable, redispersible and yet catalytically active.

4. Conclusions

Intrazeolite cobalt(0) nanoclusters were easily prepared by the ion-exchange of Co^{2+} ions with the extraframework Na^+ ions in zeolite-Y followed by the reduction of Co^{2+} ions in the supercages of zeolite-Y with sodium borohydride in aqueous solution at room temperature. The prepared intrazeolite cobalt(0) nanoclusters were used as catalyst for hydrogen generation from the hydrolysis of sodium borohydride in both aqueous and basic solutions. Hydrogen generation from the hydrolysis of sodium borohydride was studied depending on the cobalt loading of zeolite-Y, catalyst concentration, substrate concentration, temperature and basicity of the medium. A kinetic study shows that the catalytic hydrolysis of sodium borohydride is first order with respect to cobalt concentration and zero order with respect to $NaBH_4$ concentration. The high catalytic activity and long life time of intrazeolite cobalt(0) nanoclusters in the hydrolysis of sodium borohydride in basic solution can be attributed to the small size of the nanoclusters encapsulated in the cavities of zeolite-Y and their accessibility in the cages of zeolite as they interact only on one side with internal surface of zeolite. That the channels of zeolite-Y remain open is a propensity of the catalytic reactions, which do not produce any substance blocking the cage apertures of the host material.

Intrazeolite cobalt(0) nanoclusters provide 36,000 turnovers and a turnover frequency up to 880 mol H_2 (mol Co)$^{-1}$ h^{-1} in the hydrolysis of sodium borohydride solution in the presence of sodium hydroxide (10 wt.% NaOH) at room temperature. This is a record turnover number for the catalytic hydrolysis of sodium borohydride in basic solution [28]. That the intrazeolite cobalt(0) nanoclusters catalysts operate also in basic solution is of practical importance since the catalytic hydrolysis of sodium borohydride is usually performed in the presence of sodium hydroxide for hydrogen generation in the fuel cell applications in order to suppress the self-hydrolysis.

Acknowledgements

Partial support by Turkish Academy of Sciences and METU-DPT-OYP is acknowledged. M.R. thanks the TUBITAK-BIDEB (The Scientific and Technological Research Council of Turkey-The Department of Science Fellowships and Grant Programs) for the scholarship.

References

[1] Basic Research Needs for the Hydrogen Economy, Report of the Basic Energy Sciences Workshop on Hydrogen Production, Storage and Use, May 13–15, 2003, Office of Science, U. S. Department of Energy, www.sc.doe.gov/bes/hydrogen.pdf.
[2] Annual Energy Outlook 2005 with Projections to 2025, Energy Information Administration, February 2005, www.eia.doe.gov/oiaf/aeo/pdf/0383(2005).pdf.
[3] J. Turner, G. Sverdrup, K. Mann, P.G. Maness, B. Kroposki, M. Ghirardi, R.J. Evans, D. Blake, Int. J. Energy Res. 32 (2008) 379–407.
[4] IAC Report, Lighting the Way Towards a Sustainable Energy Futures, Interacademy Council, Amsterdam, 2007.
[5] (a) D.A.J. Rand, R.M. Dell, J. Power Sources 144 (2005) 568–578;
(b) J. Zhang, T.S. Fisher, J.P. Gore, D. Hazra, P.V. Ramachandran, Int. J. Hydrogen Energy 31 (2006) 2292–2298.
[6] Y. Shang, R. Chen, R. Thring, World J. Eng. 2 (2005) 1–9.
[7] (a) V.C.Y. Kong, F.R. Foulkes, D.W. Kirk, J.T. Hinatsu, Int. J. Hydrogen Energy 24 (1999) 665–675;
(b) D. Xu, H. Zhang, W. Ye, Catal. Commun. 8 (2007) 1767–1771.
[8] J. Lee, K.Y. Kong, C.R. Jung, E. Cho, S.P. Yoon, J. Han, T.G. Lee, S.W. Nam, Catal. Today 120 (2007) 305–310.
[9] H.I. Schlesinger, H.C. Brown, A.B. Finholt, J.R. Gilbreath, H.R. Hockstra, E.K. Hyde, J. Am. Chem. Soc. 75 (1953) 215–219.
[10] M.M. Kreevoy, R.W. Jacobson, Ventron Alembic 15 (1979) 2–3.
[11] S.C. Amendola, J.M. Janjua, N.C. Spencer, M.T. Kelly, P.J. Petillo, S.L. Sharp-Goldman, M. Binder, Int. J. Hydrogen Energy 25 (2000) 969–975.
[12] (a) R.E. Davis, C.G. Swain, J. Am. Chem. Soc. 82 (1960) 5950–5951;
(b) A. Levy, J.B. Brown, C.J. Lyons, Ind. Eng. Chem. 52 (1960) 211–214;
(c) H.C. Brown, C.A. Brown, J. Am. Chem. Soc. 84 (1962) 1493–1494;
(d) R.E. Mesmer, W.L. Jolly, Inorg. Chem. 1 (1962) 608–612;
(e) J.A. Gardiner, J.W. Collatt, J. Am. Chem. Soc. 86 (1964) 3165–3166;
(f) J.A. Gardiner, J.W. Collatt, J. Am. Chem. Soc. 87 (1965) 1692–1700;
(g) B. Sen, C.M. Kaufman, J. Chem. Soc., Dalton Trans. (1985) 307–313;
(h) J.H. Kim, H. Lee, S.C. Han, H.S. Kim, M.S. Song, J.Y. Lee, Int. J. Hydrogen Energy 29 (2004) 263–267;
(i) J.H. Kim, K.T. Kim, Y.M. Kang, S.K. Kim, M.S. Song, Y.J. Lee, J.Y. Lee, J. Alloys Compd. 379 (2004) 222–227;
(j) M. Chatenet, F. Micoud, I. Roche, E. Chainet, Electrochim. Acta 51 (2006) 5459–5467;
(k) K.W. Cho, H.S. Kwon, Catal. Today 120 (2007) 298–304;
(l) W. Ye, H. Zhang, D. Xu, L. Ma, B. Yi, J. Power Sources 164 (2007) 544–548;
(m) H. Zhang, B. Yi, C. Wu, Catal. Today 93 (2004) 477–483;
(n) N. Patel, G. Guella, A. Kale, A. Miotello, B. Patton, C. Zanchetta, L. Mirenghi, P. Rotolo, Appl. Catal. A 323 (2007) 18–24;
(o) N. Patel, G. Guella, A. Kale, A. Miotello, B. Patton, C. Zanchetta, R. Fernandes, J. Phys. Chem. C 112 (2008) 6968–6976;
(p) E. Keçeli, S. Özkar, J. Mol. Catal. A: Chem. 286 (2008) 87–91;
(r) R.P. Alonso, A. Sicurelli, E. Callone, G. Carturan, R. Raj, J. Power Sources 165 (2007) 315–323;
(s) G. Guella, C. Zanchetta, B. Patton, A. Miotello, J. Phys. Chem. B 110 (2006) 17024–17033;
(t) J.C. Walter, A. Zurawski, D. Montgomery, M. Thomburg, S. Pevankar, J. Power Sources 179 (2008) 335–339;
(u) J.H. Park, P. Shakkthievel, H.J. Kim, M.K. Han, J.H. Jang, Y.R. Kim, Y.G. Shul, H.S. Kim, Int. J. Hydrogen Energy 33 (2008) 1845–1852;
(v) U.B. Demirci, F. Garin, Catal. Commun. 9 (2008) 1167–1172.
[13] Y. Kojima, K.I. Suzuki, K. Fukumoto, M. Sasaki, T. Yamamoto, Y. Kawai, H. Hayashi, Int. J. Hydrogen Energy 27 (2002) 1029–1034.
[14] (a) M. Zahmakıran, S. Özkar, J. Mol. Catal. A: Chem. 258 (2006) 95–103;
(b) C.L. Hsueh, C.Y. Chen, J.R. Ku, S.F. Tsai, Y.Y. Hsu, F.H. Tsau, M.S. Jeng, J. Power Sources 177 (2008) 485–492.
[15] P. Krishnan, T.H. Yang, W.Y. Lee, C.S. Kim, J. Power Sources 143 (2005) 17–23.
[16] I.I. Korobov, N.G. Mozgina, L.N. Blinova, Kinet. Catal. 36 (1995) 380–384.
[17] (a) B.H. Liu, Z.P. Li, S. Suda, J. Alloys Compd. 415 (2006) 288–293;
(b) K.S. Eom, K.W. Cho, H.S. Kwon, J. Power Sources 180 (2008) 484–490;
(c) D. Xu, P. Dai, X. Liu, C. Cao, Q. Guo, J. Power Sources 182 (2008) 616–620;
(d) C.H. Liu, B.H. Chen, C.L. Hsueh, J.R. Ku, M.S. Jeng, F. Tsau, Int. J. Hydrogen Energy 34 (2009) 2153–2163.
[18] (a) D. Hua, Y. Hanxi, A. Xinping, C. Chuansin, Int. J. Hydrogen Energy 28 (2003) 1095–1100;
(b) A.B. Dai, Y. Liang, P. Wang, X.D. Yao, T. Rufford, M. Lu, H.M. Cheng, Int. J. Hydrogen Energy 33 (2008) 4405–4412.
[19] (a) C. Wu, F. Wu, Y. Bai, B. Yi, H. Zhang, Mater. Lett. 59 (2005) 1748–1751;
(b) P. Krishnan, S.G. Advani, A.K. Prasad, Int. J. Hydrogen Energy 33 (2008) 7095–7102;
(c) P. Krishnan, S.G. Advani, A.K. Prasad, Appl. Catal. B 86 (2009) 137–144.
[20] J. Zhao, H. Ma, J. Chen, Int. J. Hydrogen Energy 32 (2007) 4711–4716.
[21] (a) S. Özkar, M. Zahmakıran, J. Alloys Compd. 404–406 (2005) 728–731;
(b) Ö. Metin, S. Özkar, Int. J. Hydrogen Energy 32 (2007) 1707–1715.
[22] (a) S. Özkar, R.G. Finke, J. Am. Chem. Soc. 124 (2002) 5796–5810;
(b) S. Özkar, R.G. Finke, Langmuir 18 (2002) 7653–7662;
(c) S. Özkar, R.G. Finke, Langmuir 19 (2003) 6247–6260.
[23] (a) Q. Tang, Q. Zhang, P. Wang, Y. Wang, H. Wan, Chem. Mater. 16 (2004) 1967–1976;
(b) A. Seidel, J. Loos, B. Boddenberg, J. Mater. Chem. 9 (1999) 2495–2498.
[24] (a) Y. Sun, T. Sun, K. Seff, Chem. Rev. 94 (1994) 857–870;
(b) R. Ryoo, S. June-Cho, C. Pak, J. Guk-Kim, S. Ki-Ihm, J. Yong-Lee, J. Am. Chem. Soc. 114 (1992) 76–82;
(c) L. Guczi, I. Kiricsi, Appl. Catal. A 186 (1999) 375–394;
(d) L. Guczi, A. Beck, D. Horvath, Top. Catal. 19 (2002) 157–163.
[25] (a) S.T. Homeyer, W.M.H. Sachtler, J. Catal. 117 (1989) 91–101;
(b) M.S. Tzou, B.K. Teo, W.M.H. Sachtler, J. Catal. 113 (1988) 220–235;
(c) A. de Mallmann, D.J. Barthomeuf, J. Chim. Phys.-Chim. Biol 87 (1990) 535;
(d) J. de Graaf, A.J. van Dillen, K.P. de Jong, D.C. Koningsberger, J. Catal. 203 (2001) 307–321;
(e) Q. Tang, Y. Wang, Q. Zhang, H. Wan, Catal. Commun. 4 (2003) 253–258.
[26] (a) S.U. Jeong, E.A. Cho, S.W. Nam, I.H. Oh, U.H. Jung, S.H. Kim, Int. J. Hydrogen Energy 32 (2007) 1749–1754;
(b) H. Li, Y. Wu, H. Luo, M. Wang, Y. Xu, J. Catal. 214 (2003) 15–25;
(c) N. Patel, R. Fernandes, A. Miotello, J. Power Sources 188 (2009) 411–420.
[27] (a) G.N. Glavee, K.J. Klabunde, C.M. Sorensen, G.C. Hadjapanayis, Langmuir 8 (1992) 771–773;
(b) G.N. Glavee, K.J. Klabunde, C.M. Sorensen, G.C. Hadjapanayis, Langmuir 9 (1993) 162–169;
(c) G.N. Glavee, K.J. Klabunde, C.M. Sorensen, G.C. Hadjapanayis, Inorg. Chem. 32 (1993) 474–477;
(d) Q. Tang, Q. Zhang, P. Wang, Y. Wang, H. Wan, Microporous Mesoporous Mater. 86 (2005) 38–49.
[28] M. Zahmakıran, S. Özkar, Langmuir 24 (2008) 7065–7067.
[29] D.W. Breck, Zeolite Molecular Sieves, Wiley, New York, 1984.
[30] A.B. Mandale, S. Badrinarayanan, S.K. Date, A.P.B. Sinha, J. Electron Spectrosc. Relat. Phenom. 33 (1984) 61–72.
[31] (a) G. Schmid, Clusters and Colloids: From Theory to Applications, VCH Publishers, New York, 1994;
(b) L. Guczi, D. Bazin, Appl. Catal. A 188 (1999) 163–174;
(c) Y.X. Jiang, W.Z. Weng, D. Si, S.G. Sun, J. Phys. Chem. B 109 (2005) 7637–7642;
(d) A. Fukuoko, N. Higashimoto, Y. Sakamoto, S. Inagaki, Y. Fukushima, M. Ichikawa, Top. Catal. 18 (2002) 73–78;
(d) K. Okitsu, A. Yue, S. Tanabe, H. Matsumoto, Bull. Chem. Soc. Jpn. 75 (2002) 449–455;
(e) M. Zahmakiran, S. Özkar, Langmuir 25 (2009) 2667–2678.
[32] L.E. Klebanoff, D.G. Van Campen, R.J. Pouliot, Phys. Rev. B 49 (1994) 2047–2057.
[33] (a) P.P. Knops-Gerrits, D.E. De Vos, E.J.P. Feijen, P.A. Jacobs, Microporous Mater. 8 (1997) 3–17;
(b) C. Bremard, M. Le Maire, J. Phys. Chem. 97 (1993) 9695–9702;
(c) P.P. Knops-Gerrits, M. Cuypers, Stud. Surf. Sci. Catal. 142 (2002) 263.
[34] D. Gallant, M. Pezolet, S. Simard, J. Phys. Chem. B 110 (2006) 6871–6880.
[35] R.S.H. Mikhail, S. Brunauer, E.E. Bodor, J. Colloid Interface Sci. 26 (1968) 45.
[36] J.C. Ingersoll, N. Mani, J.C. Thenmozhiyal, A. Muthaiah, J. Power Sources 173 (2007) 450–457.
[37] C.A. Jaska, T.J. Clark, S.B. Clendenning, D. Grozea, A. Turak, Z.H. Lu, I. Manners, J. Am. Chem. Soc. 127 (2005) 5116–5124.
[38] T.J. Clark, G.R. Whittell, I. Manners, Inorg. Chem. 46 (2007) 7522–7527.
[39] H.B. Dai, Y. Liang, P. Wang, H.M. Chang, J. Power Sources 177 (2008) 17–23.
[40] S.C. Amendola, S.L. Sharp-Goldman, M.S. Janjua, M.T. Kelly, P.J. Petillo, M. Binder, J. Power Sources 85 (2000) 186–189.
[41] U.B. Demirci, F. Garin, J. Mol. Catal. A: Chem. 279 (2008) 57–62.
[42] N. Patel, B. Patton, C. Zanchetta, R. Fernandes, G. Guella, A. Kale, A. Miotello, Int. J. Hydrogen Energy 33 (2008) 287–292.
[43] Z. Liu, B. Guo, S.H. Chan, E.H. Tang, L. Hong, J. Power Sources 176 (2008) 306–311.
[44] Q. Zhang, Y. Wu, X. Sun, J. Ortega, Ind. Eng. Chem. Res. 46 (2007) 1120–1124.
[45] M. Mitov, R. Rashkov, N. Atanassov, A. Zielonka, J. Mater. Sci. 42 (2007) 3367–3372.
[46] Z.S. Zhang, W.N. Delgass, T.S. Fisher, J.P. Gore, J. Power Sources 164 (2007) 772–781.